eNeuro

Research Article: New Research | Sensory and Motor Systems

Minute Impurities Contribute Significantly to Olfactory Receptor Ligand Studies: tales from Testing the Vibration Theory.

Minute impurities distort olfactory receptor responses

M. Paoli[1,2,*], D. Münch[1,*], A. Haase[2], E. Skoulakis[3], L. Turin[3] and C. G. Galizia[1]

[1]Neurobiology, University of Konstanz, Konstanz, 78457, Germany

[2]Department of Physics and Center for Mind/Brain Sciences, University of Trento, Povo, TN 38123, Italy

[3]Division of Neuroscience, Biomedical Sciences Research Centre "Alexander Fleming, Vari, 16672, Greece"

Cite as: eNeuro 2017; 10.1523/ENEURO.0070-17.2017

Alerts: Sign up at eneuro.org/alerts to receive customized email alerts when the fully formatted version of this article is published.

1   **Manuscript Title (50 word maximum)**

2 Minute impurities contribute significantly to olfactory receptor ligand studies: tales from testing the

3 vibration theory.

4

5   **Abbreviated Title (50 character maximum)**

6 Minute impurities distort olfactory receptor responses

7

8   **List all Author Names and Affiliations in order as they would appear in the published article**

9 Paoli M*[1,2], Münch D*[1], Haase A[2], Skoulakis E[3], Turin L[3], CG Galizia[1, 4]

10 * contributed equally to this work

11 [1]: Neurobiology, University of Konstanz, 78457 Konstanz, Germany.

12 [2]: Department of Physics and Center for Mind/Brain Sciences, University of Trento, Povo (TN), 38123,

13 Italy

14 [3]: Division of Neuroscience, Biomedical Sciences Research Centre "Alexander Fleming," 16672 Vari,

15 Greece

16 [4]: correspondence to: galizia@uni.kn

17

18

19   **Author Contributions:**

20   All authors designed research. MP and DM performed research. MP, DM and CGG analyzed

21 data. CGG wrote the paper, all authors edited the paper.

22

23   **Correspondence should be addressed to (include email address)**

24 CGG, galizia@uni.kn

25

26   Number of Figures: 4

27   Number of Tables: 0

28   Number of Multimedia: 0

29   Number of words for Abstract: ##

30   Number of words for Significance Statement: ##

31   Number of words for Introduction: ##

32   Number of words for Discussion: ##

33

34   **Acknowledgements**

36   **Conflict of Interest**

37 Authors report no conflict of interest

38

39   **Funding sources**

43 # Minute impurities contribute significantly to olfactory receptor ligand

44 # studies: tales from testing the vibration theory.

45 ## Abstract

46 Several studies have attempted to test the vibrational hypothesis of odorant receptor activation in

47 behavioral and physiological studies using deuterated compounds as odorants. The results have been

48 mixed. Here we attempted to test how deuterated compounds activate odorant receptors using

49 calcium imaging of the fruit fly antennal lobe. We found specific activation of one area of the AL

50 corresponding to inputs from a specific receptor. However, upon more detailed analysis, we

51 discovered that an impurity of 0.0006% ethyl acetate in a chemical sample of benzaldehyde-d_5 was

52 entirely responsible for a sizable odorant-evoked response in *Drosophila melanogaster* olfactory

53 receptor cells expressing dOr42b. Without gas chromatographic purification within the experimental

54 setup, this impurity would have created a difference in the responses of deuterated and non-

55 deuterated benzaldehyde, suggesting that dOr42b be a vibration sensitive receptor, which we show

56 here not to be the case. Our results point to a broad problem in the literature on use of non GC-pure

57 compounds to test receptor selectivity, and we suggest how the limitations can be overcome in

58 future studies.

59 ## Significance statement

60 How exactly odorant receptors create selectivity for some odorants against the vast number of

61 alternatives remains as yet unclear, and is generally probed by measuring responses to different

62 substances. Chemical senses are highly sensitive to minute amounts of odorants in the environment.

63 Therefore, when testing the responses of olfactory receptors, substances of highest purity are used,

64 generally 95% or 99%, i.e. with impurities of 5% or 1%. The authors report a case where an impurity

65 of 0.0006% was sufficient to explain the full response of an olfactory receptor in a test situation. The

66   authors demostrate why all experiments investigating the selectivity of odor receptors have to be

67   performed with gas-chromatography-purified odors to eliminated potential impurity artifacts.

Introduction

68

69   How odorants interact with receptors remains elusive: a key-lock system has been proposed early on

70   (Amoore, 1963), but this does not yet explain how a transduction cascade is activated (i.e. how the

71   fitting key is turned inside the lock). Different mechanisms have been proposed, including the

72   involvement of metal ions creating metalloproteins (Turin, 1996; Wang et al., 2003; Duan et al.,

73   2012), and electron tunneling in resonance with molecular vibrations (Turin, 1996).

74   Crystallography is the most direct approach to studying receptor-ligand interaction, but only few

75   examples exist, including the cholinergic receptor (Warne et al., 2008) and photoreceptors

76   (Palczewski et al., 2000; Standfuss et al., 2011). No olfactory receptor has been analyzed in this way

77   yet. An alternative approach relies on modeling the binding pocket (Guo & Kim, 2010). Here, large

78   sets of odor-response data are necessary, ideally recorded in a hypothesis-free approach. However,

79   in both cases, the result consists in an estimate for the shape of the binding pocket, but not yet in a

80   mechanism of how the receptor is activated. Dedicated, hypothesis-driven studies are better suited

81   to this end: if vibrations are to be tested, the task would be to find a receptor that does respond to

82   one vibration frequency, and not to another.

83   Deuterated substances offer an ideal possibility to test whether molecular vibrations contribute to

84   activating olfactory receptors. When hydrogen (H) is replaced by deuterium (D) in a molecule, the

85   chemical properties do not change, but a new vibration range is added. For example, the C-D bond

86   has a vibration at around 2150 cm^{-1}, which is not present in a molecule lacking deuterium. Deuterium

87   can also add other vibrations: the ring in benzaldehyde-d_5 creates a collective out-of-plane vibration

88   around 550 cm^{-1} (Klika, 2013; Paoli et al., 2016). The logic of these experiments is that, if an animal

89   can differentiate between a deuterated and a non-deuterated substance that otherwise are equal

90   (say, between benzaldehyde and its deuterated form, which smell almond-like to humans), vibrations

91   must play a role, since that is the main physical factor that differentiates the two odorant stimuli.

92   This hypothesis has been tested in a variety of studies, using humans, fruit-flies, honeybees and

93   other animals, and using paradigms including behavior and physiology (Haffenden et al., 2001; Keller

94   and Vosshall, 2004; Franco et al., 2011; Bittner et al., 2012; Gane et al., 2013; Gronenberg et al.,

95   2014; Paoli et al., 2016). However, the results are contradictory, since some studies argue for and

96   others against vibrations, leading to controversial discussions (Solov'yov et al., 2012; Block et al.,

97   2015).

98   Another aspect to be considered is that olfactory receptor gene families are highly divergent. Even

99   within single species, there are several unrelated families of olfactory receptors: in mammals, at least

100   6 different families have been reported (Fleischer et al., 2009; Greer et al., 2016), in insects IRs and

101   ORs are two distinct families (Silbering et al., 2011). A hypothesis would be that a single family, or

102   even a particular receptor, could use one or more activation mechanisms – e.g. vibration detection,

103   size, etc. – while others could respond to different odorant properties. Therefore, studying how

104   responses to deuterated substances differ from non-deuterated substances is best done on single

105   receptor types, rather than the whole olfactory system.

106   Receptors have broad or narrow response profiles (Galizia et al., 2010; Münch and Galizia, 2016), but

107   even the latter respond to minor ligands when presented at a sufficiently high concentration.

108   Optimal concentrations for eliciting responses in receptors can span many orders of magnitude. For

109   example, Or22a in *Drosophila* has an EC50 (effective concentration/dilution for half-maximal

110   response) of $10^{-6.9}$ for methyl hexanoate, and an EC50 of $10^{-4.2}$ for isoamyl acetate, and both dilutions

111   create concentrations that *Drosophila* is easily exposed to in a natural environment (Pelz et al.,

112   2006). The difference of several orders of magnitude between these two stimuli means that small

113   amounts of impurities can have a strong effect on odor responses. Examples of single sensillum

114   recordings where the responses were entirely due to impurities in commercial odorant sources have

115   been published for moths (Stranden et al., 2003).

116   In this study, we combined these thoughts in an attempt to test the vibration theory of olfaction.

117   First, we searched for a single receptor type that would show differential responses between

118   deuterated and non-deuterated substances, and found one with an apparent difference. Results such

119   as these have been published as evidence in favor of the vibrational theory. Next, we recorded the

120   odorants' responses via a gas chromatograph, and found that in our case the difference was due to a

121   minute contaminant (0.0006%, or 6 ppm). Finally, we show that adding the contaminant to the non-

122   deuterated substances elicits a response similar to the one seen for for the deuterated substance.

123   We conclude that the results do not support the vibrational theory. Importantly, however, they do

124   not disprove it either – rather, they show how important it is not only to use substances of highest

125   purity, but indeed to purify substances on the spot using gas chromatography. As a corollary, the

126   validity of data in studies on receptor-ligand interaction in general that have not used appropriate

127   purification techniques needs to be reconsidered.

Materials and methods

128

Animals

129

130   All recordings were performed on female *Drosophila melanogaster* fruit flies expressing either the

131   calcium reporter G-CaMP5 (Akerboom et al., 2012) under the control of the olfactory co-receptor

132   Orco (Orco-Gal4>UAS-GCaMP5), or expressing the reporter GCaMP6m (Chen et al., 2013) in Or42b

133   olfactory receptor neurons (Or42b-Gal4>UAS-GCaMP6m). Calcium reporter driver lines were

134   obtained from the Bloomington Stockcenter (Bloomington, USA; RRID:BDSC_42038 and

135   RRID:BDSC_42748), Or42b-Gal4 (likely RRID:BDSC_9972) and Orco-Gal4 (likely RRID:BDSC_26818)

136   flies were kindly provided by Veith Grabe and Silke Sachse, MPI for Chemical Ecology, Jena, Germany.

137   Flies were kept at 25°C in a 12/12 light/dark cycle at 60-70% RH. Animals were reared on standard

138   medium (100 ml contain: 2.2 g yeast, 11.8 g of sugar beet syrup, 0.9 g of agar, 5.5 g of cornmeal, 1 g

139   of coarse cornmeal and 0.5 ml of propionic acid).

Animal preparation

140

141 For antennal lobe recordings flies were anesthetized on ice and placed into a custom-made holder.

142 The head was fixed to the holder with low-melting wax, the antennae were gently pulled forward

143 with a thin copper wire, and a polyethylene foil was placed on the head and sealed with

144 bicomponent silicon (Kwik-Sil, WPI). A small window was cut through the foil and head cuticle, and

145 the exposed brain was covered in saline solution (130 mM NaCl, 5 mM KCl, 2 mM $MgCl_2$, 2 mM $CaCl_2$,

146 36 mM sucrose, 5 mM Hepes, pH 7.3, all chemicals from Sigma-Aldrich). Glands and tracheae were

147 removed to allow optical access to the antennal lobe. For antenna recordings flies were mounted in

148 custom-made holders. The head was fixed to the holder with a drop of low-melting wax. A half

149 electron-microscopy grid was placed on top of the head, stabilizing the antenna by touching the 2nd,

150 but not the 3rd antennal segment. For details on the antennal lobe preparation, see (Silbering and

151 Galizia, 2007; Silbering et al., 2008). For details on the antennal preparation, see (Münch and Galizia,

152 2016).

Odorant preparation

153

154 Benzaldehyde-2,3,4,5,6-d_5 was purchased at CDN isotopes (CAS: 14132-51-5, Lot #: I240P14, isotopic

155 enrichment 99%). All other odorants were purchased at Sigma-Aldrich in the highest purity available.

156 Odorants used were: benzaldehyde (CAS: 100-52-7, Lot #: STBD7798V, ≥99.5%), E2-hexenal (CAS:

157 6728-26-3, Lot #: S28442V, 98%), ethyl acetate (CAS: 141-78-6, Lot #: BCBR9070V, ≥99.9%), ethyl

158 propionate (CAS: 105-37-3, Lot #: BCBL5952V, ≥99.7%), ethyl butyrate (CAS: 105-54-4, Lot #:

159 BCBR7796V, ≥99.5%), propyl acetate (CAS: 109-60-4, Lot #: BCBL5998V, ≥99.7%), ethyl (S)-(+)-3-

160 hydroxybutyrate (CAS: 56816-01-4, Lot #: BCBM4473V, 99%), 3-hexanone (CAS: 589-38-8, Lot #:

161 BCBJ8237V, 98%), beta-butyrolactone (CAS: 3068-88-0, Lot #: MKBJ3709V, 98%), (±)-2-Hexanol (CAS:

162 626-93-7, Lot #: MKBJ5626V, ≥ 98%), methyl acetate (CAS: 79-20-9 , Lot #: BCBN9450V, ≥99.9%), 3-

163 penten-2-one (CAS: 625-33-2, Lot #: SHBC5346V, ≥70%). Pure substances were diluted in mineral oil

164 (Sigma-Aldrich) at the indicated dilutions, and covered with Argon (Sauerstoffwerk Friedrichshafen

165 GmbH, Germany) to avoid oxidation. Dilutions were prepared in 5 ml mineral oil (CAS: 8042-47-5;

Minute impurities contribute to olfactory receptor responses   6

166   Acros Organics, Belgium) in 20ml head space vials covered with pure nitrogen to avoid oxidation

167   (Sauerstoffwerk Friedrichshafen GmbH, Germany) and immediately sealed with a Teflon septum

168   (Axel Semrau, Germany).

169   Odorant delivery

170   A GC-FID system (TRACE GC Ultra, Thermo Fisher Scientific, USA) in conjunction with an autosampler

171   (PAL, CTC Switzerland) was used for odorant delivery. The autosampler was used to either inject

172   headspace samples into the GC, or directly to the antenna, bypassing the GC system. For GC-coupled

173   antenna measurements, 1 ml of headspace was injected into the GC at split mode with the injector

174   temperature set to 200°C, the split flow to 15 ml/min and the split ratio to 10. The GC was equipped

175   with an Optima® 5 MS 30 m × 0.25 mm × 0.25 µm column (Macherey-Nagel, Germany). The flow of

176   the carrier gas helium was set to 1.5 ml/min. The oven was held at 60°C for 1 min, then the

177   temperature was increased to 200°C at 20°C/min, the final temperature was again held for 1 min.

178   One half of the eluate was directed to the FID detector (set to 200°C) and the other half to the

179   animal's antenna via an olfactory detection port (either ODP3, Gerstel, Germany, or Semrau,

180   Germany). GC-FID trace and antennal trace alignment was calibrated using the response peak to

181   ethyl acetate. FID data was recorded using Xcalibur software (Thermo Fisher Scientific,

182   Massachusetts, USA). After each injection the syringe was washed with n-pentane (Merk KgaA,

183   Germany), heated and flushed with clean air. For direct stimulations (bypassing the GC) a head space

184   of 2 ml was injected in two 1 ml portions at time points 6 s and 8.5 s with an injection speed of 1 ml/s

185   into a continuous flow (60 ml/min) of purified air (two one-second stimuli with 1.5 s gap). Stimuli

186   arrived at the antenna with ~750 ms delay due to delays in the autosampler and the flow. Therefore,

187   stimulus onset was determined as 6.75 s and 9.25 s. In the Figures, t = 0 was set to correspond to the

188   first stimulus onset. The stimulus was directed at the antenna of the animal via a Teflon tube (inner

189   diameter 2 mm, length 39.5 cm, with the exit positioned ~2 mm from the antenna). Between

190   successive stimuli, the syringe was flushed with clean air. The inter-trial interval was approximately 2

191   min. For each animal, prior to odor delivery, responses to clean air and to mineral oil only were

192   tested as controls.

193   Calcium imaging

194   Calcium imaging of antenna (dendrites and somata of olfactory sensory neurons) and antenna lobes

195   (axon terminals of olfactory sensory neurons) was performed on a setup consisting of a fluorescence

196   microscope (BX51WI, Olympus, Japan) equipped with a 20× water immersion objective for antennal

197   lobe recordings (Olympus XLUM Plan FI 20×/0.95) or with a 50× air lens without cover slip correction

198   for antenna recordings (Olympus LM Plan FI 50×/0.5). Images were recorded with a CCD camera

199   (SensiCam, PCO, Germany) with 4 × 4 pixel on-chip binning, which resulted in 160 × 120 pixel sized

200   images for AL recordings or with 8 × 8 pixel on-chip binning, which resulted in 80 × 60 pixel sized

201   images for antenna recordings. For AL measurements we recorded each stimulus for 20 s at a rate of

202   4 Hz using TILLvisION (TILL Photonics, Germany), GC-coupled antenna imaging was performed at 1 Hz

203   for 9 min. A monochromator (Polychrome V, TILL Photonics, Germany) produced excitation light at a

204   wavelength of 470 nm which was directed onto the antenna via a 500 nm low-pass filter and a 495

205   nm dichroic mirror. Emission light was filtered through a 505 nm high-pass emission filter.

206   Benzaldehyde-h/d_5 antennal lobe measurements were performed in a total of N=6 animals

207   expressing Orco>GCaMP5 (Fig. 1A & C), and N=3 animals expressing Or42b>GCaMP6m (Fig. 1 D). GC-

208   coupled antenna recordings of benzaldehyde-h/d_5 were performed in a total of N=3 animals

209   expressing Or42b>GCaMP6m (Fig. 1E & Fig. 3C). Responses to blended benzaldehyde-h with

210   increasing concentrations of "contaminant" were measured in N=3 animals expressing

211   Or42b>GCaMP6m (Fig. 4). The GC-coupled antenna recordings in Fig. 2 are based on data from N=5

212   animals expressing Or42b>GCaMP6m, dose-response data in Fig. 3A & B are based on data from N=5

213   animals expressing Or42b>GCaMP6m.

214   Data analysis

215   Custom made R and Python scripts were used for data analysis. The Python-based ILTIS software

216   (Raiser et al., unpublished; https://github.com/grg2rsr/ILTIS) was used for calcium imaging

217   visualization, baseline subtraction and normalization. Relative fluorescence change was calculated as

218    $\Delta F/F = (F_i - F_0)/F_0$ with F_i being the fluorescence at frame i and F_0 being the mean fluorescence before

219   stimulus onset. GC-antenna recordings were corrected for dye bleaching by fitting an exponential

220   decay function of the form $A * e^{-x/B} + C$ to each response trace, leaving out the parts of the trace

221   where activity was recorded. Responses were calibrated across animals to the first response peak of

222   ethyl butyrate, most likely $10^{-5.6}$ ethyl acetate (Fig. 3).

223   Dose-response curve (Fig. 3B) was obtained by least-squares fitting responses R at concentrations c

224   with a sigmoidal logistic function of the form $R = R_{max} * \frac{1}{1+e^{-h*(c-EC50)}}$, with R_{max} corresponding to

225   maximum response asymptote, $EC50$ the half-effective dilution, and h the steepness (reminiscent of

226   the Hill-coefficient).

227   Results

228   We used calcium imaging of the antennal lobe in the fruit fly *Drosophila melanogaster* to record

229   odorant evoked activity patterns. Specifically, we were interested in differences between the

230   responses to benzaldehyde-h (normal benzaldehyde), and benzaldehyde-d_5, where the hydrogen

231   atoms of the benzene ring were replaced by deuterium. We expressed the calcium sensor GCaMP5

232   (Akerboom et al., 2012) under the control of the olfactory coreceptor Orco (GAL4-Orco > UAS-

233   GCaMP5), and stimulated with two 1 s stimuli with a 1.5 s gap in between. Both normal and

234   deuterated benzaldehyde elicited similar responses throughout the antennal lobe, with the strongest

235   response in the dorsolateral area (area R1 in Fig. 1A).

236   However, we also noted a dorsomedial area with clearly different responses to the two isotopomers,

237   with apparent odorant elicited responses to benzaldehyde-d_5, and no apparent responses to

238   benzaldehyde-h (area R2 in Fig. 1A). Therefore, we focused on this area because it could provide an

239   important, clear test of the vibrational hypothesis. Using the antennal lobe atlas for *Drosophila*

240   (Grabe et al., 2015), we identified two potential candidates for this area: glomerulus DM1,

241   innervated by Or42b, and glomerulus DL5, innervated by Or7A. To confirm the identity of the

242   putative isotope-sensitive area, we screened the DoOR database (Münch and Galizia, 2016) for two

243   odorants that induced a strong response in either the DL5 or the DM1 glomerulus. For this purpose,

244   we selected E2-hexenal (Fig. 1B) and ethyl butyrate (Fig. 1B'). E2-hexenal gave a strong response in

245   the dorsolateral area, corresponding to glomerulus DL5, which is innervated by axons from ORs

246   expressing Or7A (Fig. 1C). Ethyl butyrate elicited responses more medially, corresponding to the area

247   innervated by Or42b and Or22a (Fig. 1C). A comparison between the response patterns induced by

248   the four odorants indicated a clear overlap between the dorsomedial area of the ethyl butyrate-

249   induced signal – corresponding to glomerulus DM1 – and the benzaldehyde-d_5 responsive region

250   (dotted line in Fig. 1C). Thus, we confirmed this area to be glomerulus DM1, innervated by Or42b. We

251   then expressed the calcium sensor GCaMP6m (Chen et al., 2013) specifically in the Or42b receptor

252   neurons (Or42b-GAL4>UAS-GCaMP6m), and confirmed that Or42b responded to ethyl butyrate as

253   well as to benzaldehyde-d_5 (Fig. 1D). Responses to benzaldehyde-h, however, were inhibitory (blue

254   trace in Fig. 1D).

255   In order to show more conclusively that the response of this glomerulus was due to benzaldehyde-d_5,

256   and to exclude that minor impurities could cause this difference between the two isotopomers, we

257   coupled the imaging setup to a gas chromatograph outlet. With this experimental setup, response to

258   either benzaldehyde-h or benzaldehyde-d_5 was inhibitory at the elution time of benzaldehyde.

259   However, we found a strong excitatory response to benzaldehyde-d_5 at an earlier elution time, which

260   was not present in the benzaldehyde-h recording (Fig. 1E). These results indicated that the apparent

261   response to benzaldehyde-d_5 in Or42b was due to some contaminating trace molecules. These data

262   also suggested that the inhibitory response to benzaldehyde-d_5 (as seen in Fig. 1D) was masked by

263   the contaminating substance.

264   Next, we sought to identify the impurity. Using the DoOR database (Münch and Galizia, 2016), we

265   selected a set of best ligands for Or42b, purchased them at highest available purity, and measured

266   their chemical purity using GC-FID (red traces in Fig. 2). With the exception of 3-penten-2-one, where

267   we saw two peaks, all other substances only had a single detectable peak in the FID trace, with all

268   minor peaks in the noise range. Next, we recorded the calcium responses in Or42b to the GC eluates.

269   We found a strong response to ethyl acetate that decayed progressively after the stimulus, indicating

270   receptor saturation. Similarly, ethyl propionate, propyl acetate and ethyl (S)-(+)-3-hydroxybutyrate all

271   elicited responses that decayed slowly after the stimulus had terminated, indicating some degree of

272   saturation. Most importantly, however, we noted that ethyl propionate, ethyl butyrate, propyl

273   acetate and ethyl (S)-(+)-3-hydroxybutyrate all also elicited responses at the elution time of ethyl

274   acetate (Fig. 2). These responses indicated that ethyl acetate might have been a trace impurity in

275   these stimuli. The responses were quite different in size for the different stimuli, indicating that the

276   contamination differed in concentration. Indeed, other stimuli that we tested did not elicit any

277   response at the elution time of ethyl acetate (see, for example, the response to methyl acetate or to

278   3-hexanone in Fig. 2), indicating that these responses must have been generated by a specific

279   impurity. Other impurities also elicited responses: ethyl butyrate elicited four response peaks in

280   Or42b (Fig. 2), one with retention time corresponding to ethyl acetate, one with retention time

281   corresponding to ethyl propionate or propyl acetate, one unknown, and one corresponding to ethyl

282   butyrate itself.

283   What was the concentration of the ethyl acetate contamination in the benzaldehyde-d_5 sample? We

284   recorded a dose-response curve of ethyl acetate calcium responses in Or42b from the purified GC

285   eluate. At very low concentration, no response could be detected. With increasing concentration, the

286   response size increased, and at very high concentration the response formed a tail, with calcium

287   decreasing only slowly (red traces in Fig. 3A). Across concentrations, this yielded a sigmoidal dose

288   response curve, with half-maximal response at a dilution of $10^{-5.0}$ (Fig. 3B). We normalized these

289   responses to the ethyl acetate peak in the response to ethyl butyrate (gray trace in Fig. 3A). The

290   responses to the benzaldehyde-d_5 concentration were weaker (green traces in Fig. 3C, corresponding

291   to benzaldehyde-d_5 dilutions of 10^{-2}, light trace, and 10^{-1}, dark trace). These responses corresponded

292   to the values for ethyl acetate of $10^{-7.4}$ and $10^{-6.1}$, in good approximation of a single decadic dilution

293   step. Thus, we could quantify that a 10^{-1} dilution of benzaldehyde-d_5 contained $10^{-6.1}$ ethyl acetate,

294   while a 10^{-2} dilution contained $10^{-7.4}$ ethyl acetate, on average a $10^{-5.2}$ contamination. This

295   corresponded to an impurity of 6 ppm, or 0.0006%, which is at the low end of the detection limit of

296   gas chromatography using flame ionization detectors.

297   Could the heat in the GC cause unexpected artefacts, such as conformational changes in the

298   molecules? To exclude this possibility, and to test whether artificially adding an impurity of ethyl

299   acetate to benzaldehyde-h is sufficient to generate a response as the one that we found for

300   benzaldehyde-d_5, we generated synthetic mixtures of benzaldehyde-h with the impurity. We

301   recorded the calcium responses in Or42b>GCaMP6m antennae. Responses to benzaldehyde-h were

302   again inhibitory (trace "0" in Fig. 4). Adding increasing concentrations of ethyl acetate ranging from

303   10^{-10} to 10^{-2} led to a dose-dependent shift from the inhibitory response (traces 10^{-10} to 10^{-7} in Fig. 4)

304   to an increasingly excitatory response (traces 10^{-6} to 10^{-2} in Fig. 4), confirming that adding minute

305   amounts of ethyl acetate was sufficient to mimic the response induced by benzaldehyde-d_5.

Discussion

307   Many olfactory receptors have a broad response profile, with sensitivities ranging over many log-

308   decade concentrations. For example, the *Drosophila* receptor Or22a has a half-maximal response to

309   methyl hexanoate at a dilution of $10^{-6.9}$, and to isoamyl acetate at a dilution of $10^{-4.2}$ (Pelz et al., 2006)

310   (note that quantitative indications of concentrations depend on experiment specific settings,

311   therefore absolute values are difficult to compare between experiments. Relative values, however,

312   are comparable). Both are substances and concentrations that occur in the environment of the fruit

313   fly, therefore both are ecologically relevant. This gives an interesting twist to analyzing odorant

314 responses in a natural environment, where most stimuli are mixtures of several chemicals: a

315 response might derive from a major component, from a trace element, or both (Münch et al., 2013).

316 Here, we give an example where an impurity of 0.0006% (6 ppm) explains the full response of a

317 single receptor cell type. Given that for most substances the highest commercially available purity is

318 95% or 99%, these results are important for our interpretation of many odorant-response studies,

319 and not limited to investigating the vibrational theory. The headspace of the benzaldehyde-d_5 batch

320 that we used in our experiments had been analyzed chemically in great detail, resulting in 99.85%

321 purity, with a 0.1% impurity due to an individual contaminant, but no evidence for ethyl acetate

322 (data not shown), since the GC analysis did not reach the 0.0006% sensitivity that the natural

323 *Drosophila* receptor has. Another study used benzaldehyde-d_6, and the chemical analysis revealed

324 eight contaminants, all of which at a concentration higher than 0.0006% (Drimyli et al., 2016). Under

325 such circumstances, the contribution of ethyl acetate can easily go undetected when testing

326 deuterated benzaldehyde. Furthermore, ethyl acetate is not used in the synthesizing process of

327 benzaldehyde-d_5 (personal communication from the manufacturers), adding the additional caveat

328 that post-production impurities could be any chemical. We do not claim that any particular study

329 about the effect of deuterated substances can be explained by trace impurities. For example,

330 experiments showing learning transfer between deuterated compounds and nitriles (Franco et al.,

331 2011) are less likely to suffer from an impurity problem. We can only add a note of caution, and

332 substantiate the need for on-the-spot purification. Furthermore, trace compounds, even if they are

333 good ligands when given alone, do not always dominate the response of a receptor in a mixture: a

334 "secondary" ligand given simultaneously in a mixture could be able to obscure the response to the

335 primary ligand due to syntopic interactions (Münch et al., 2013). In such a case, the response to the

336 trace component would be visible when purified (e.g., as done here, with the GC), but it would not

337 contribute significantly to the response when given in a mixture, as contaminant.

338 Examples of highly sensitive olfactory receptors have been published previously: several moth

339 species have receptors highly sensitive and selective for (-)-germacrene-D, and give responses to

340   stimulation down to 1 ng, and 10-fold less sensitive (10 ng) to the enantiomer. In these recordings,

341   tiny amounts of (-)-germacrene-D among other substances created false positive results in

342   physiological recordings in moths (Stranden et al., 2003). In order to ensure purity of the delivered

343   stimulus, it is necessary to record from the olfactory receptor at the exit of a gas chromatographic

344   column (Stranden et al., 2003; Schubert et al., 2014). This technique has been used to identify other

345   highly selective and sensitive receptors (Stensmyr et al., 2012; Dweck et al., 2013; Ebrahim et al.,

346   2015).

347   Odors are encoded as combinatorial patterns of activated olfactory receptors (Galizia, 2014).

348   Therefore, it is necessary to measure the responses of many receptor neurons to many chemical

349   substances, an approach that has been performed in a series of screening experiments, many of

350   them in *Drosophila* (Hallem and Carlson, 2006; Kreher et al., 2008; Montague et al., 2011; Silbering et

351   al., 2011). These have been collected in a consensus data-base (Münch and Galizia, 2016) that allows

352   for computational analyses of odor coding (Boyle et al., 2013; Saberi and Seyed-allaei, 2016).

353   However, the results here add a note of caution to the reliability of large odor-response screens. Out

354   of the ten substances tested in Fig. 2 for Or42b, four (ethyl propionate, ethyl butyrate, propyl acetate

355   and ethyl(S)-(+)-3-hydroxybutyrate) gave responses not only to the main component, but also to a

356   (small) contamination with ethyl acetate. Importantly, ethyl acetate was not the only trace impurity

357   to elicit responses (see responses to 3-penten-2-one and responses to ethyl butyrate, that had two

358   more effective impurities, one putatively propyl acetate). These minute contaminations create a

359   distortion in large screening studies that is difficult to correct without reassessing all measurements

360   in a GC-coupled mode. In the specific case of Fig. 2, for example, we tested the ten best ligands

361   according to the consensus database in DoOR (Münch and Galizia, 2016). The best ligand in our data

362   was ethyl acetate (see Fig. 2). In the DoOR database ethyl acetate does not rank first, since not all

363   studies of Or42b reported ethyl acetate as the strongest ligand, and the merging algorithm in DoOR

364   is agnostic about the reliability of each study. Some of the differences, e.g. in the case of ethyl (S)-(+)-

365   3-hydroxybutyrate, may be due to differences in concentrations used across studies (most screening

366   studies do not include full concentration series). However, some "best ligands" in the database may

367   have been overvalued due to the contribution of a contaminant in the chemical sample.

368   We started this study searching for a receptor that would respond differently to a deuterated

369   substance than to the hydrogenated substance – in the case of a positive result, this would have

370   indicated that that receptor might have been sensitive to a vibration around 550 cm^{-1} or around 2150

371   cm^{-1}. While we found a receptor that responded differently to our two stimuli, we could show that

372   this difference was due not to the deuteration, but rather to a minute impurity of 0.0006%, while the

373   response to deuterated benzaldehyde was identical to the response to hydrogenated benzaldehyde

374   (Fig. 1E). By adding the impurity to benzaldehyde-h we obtained the same response as for the

375   contaminated benzaldehyde-d$_5$, confirming that the contamination was sufficient to overcome the

376   inhibitory effect of benzaldehyde-h and induce an excitatory response (Fig. 4). We can show that

377   Or42b is not responding to a vibration of 550 or 2150 cm^{-1}, and it is unlikely that any of the ORs

378   labeled in an Orco line are responding to that vibration in benzaldehyde-d$_5$ either, because such a

379   difference would have been seen in our measurements of the antennal lobe (Fig. 1C). These results

380   do not exclude that there might be receptors in *Drosophila* (or other species) that have evolved a

381   mechanism for using molecular vibration to support response selectivity.

Acknowledgements

References

388   Akerboom J et al. (2012) Optimization of a GCaMP Calcium Indicator for Neural Activity Imaging. J
389   Neurosci 32:13819-13840.
390   Amoore JE (1963) Stereochemical Theory of Olfaction. Nature 198:271-272.

391   Bittner ER, Madalan A, Czader A, Roman G (2012) Quantum origins of molecular recognition and
392   olfaction in Drosophila. J Chem Phys 137:22A551.
393   Block E, Jang S, Matsunami H, Sekharan S, Dethier B, Ertem MZ, Gundala S, Pan Y, Li S, Li Z, Lodge SN,
394   Ozbil M, Jiang H, Penalba SF, Batista VS, Zhuang H (2015) Implausibility of the vibrational
395   theory of olfaction. Proc Natl Acad Sci U S A 112:E2766-2774.
396   Boyle SM, McInally S, Ray A (2013) Expanding the olfactory code by in silico decoding of odor-
397   receptor chemical space. Elife 2:e01120.
398   Chen TW, Wardill TJ, Sun Y, Pulver SR, Renninger SL, Baohan A, Schreiter ER, Kerr RA, Orger MB,
399   Jayaraman V, Looger LL, Svoboda K, Kim DS (2013) Ultrasensitive fluorescent proteins for
400   imaging neuronal activity. Nature 499:295-300.
401   Drimyli E, Gaitanidis A, Maniati K, Turin L, Skoulakis EM (2016) Differential Electrophysiological
402   Responses to Odorant Isotopologues in Drosophilid Antennae. eNeuro 3.
403   Duan XF, Block E, Li Z, Connelly T, Zhang J, Huang ZM, Su XB, Pan Y, Wu LF, Chi QY, Thomas S, Zhang
404   SZ, Ma MH, Matsunami H, Chen GQ, Zhuang HY (2012) Crucial role of copper in detection of
405   metal-coordinating odorants. P Natl Acad Sci USA 109:3492-3497.
406   Dweck HKM, Ebrahim SAM, Kromann S, Bown D, Hillbur Y, Sachse S, Hansson BS, Stensmyr MC (2013)
407   Olfactory Preference for Egg Laying on Citrus Substrates in Drosophila. Curr Biol 23:2472-
408   2480.
409   Ebrahim SAM, Dweck HKM, Stokl J, Hofferberth JE, Trona F, Weniger K, Rybak J, Seki Y, Stensmyr MC,
410   Sachse S, Hansson BS, Knaden M (2015) Drosophila Avoids Parasitoids by Sensing Their
411   Semiochemicals via a Dedicated Olfactory Circuit. Plos Biol 13.
412   Fleischer J, Breer H, Strotmann J (2009) Mammalian olfactory receptors. Front Cell Neurosci 3:9.
413   Franco MI, Turin L, Mershin A, Skoulakis EMC (2011) Molecular vibration-sensing component in
414   Drosophila melanogaster olfaction. P Natl Acad Sci USA 108:3797-3802.
415   Galizia CG (2014) Olfactory coding in the insect brain: data and conjectures. Eur J Neurosci 39:1784-
416   1795.
417   Galizia CG, Münch D, Strauch M, Nissler A, Ma SW (2010) Integrating Heterogeneous Odor Response
418   Data into a Common Response Model: A DoOR to the Complete Olfactome. Chem Senses
419   35:551-563.
420   Gane S, Georganakis D, Maniati K, Vamvakias M, Ragoussis N, Skoulakis EMC, Turin L (2013)
421   Molecular Vibration-Sensing Component in Human Olfaction. Plos One 8.
422   Grabe V, Strutz A, Baschwitz A, Hansson BS, Sachse S (2015) Digital In Vivo 3D Atlas of the Antennal
423   Lobe of Drosophila melanogaster. J Comp Neurol 523:530-544.
424   Greer PL, Bear DM, Lassance JM, Bloom ML, Tsukahara T, Pashkovski SL, Masuda FK, Nowlan AC,
425   Kirchner R, Hoekstra HE, Datta SR (2016) A Family of non-GPCR Chemosensors Defines an
426   Alternative Logic for Mammalian Olfaction. Cell 165:1734-1748.
427   Gronenberg W, Raikhelkar A, Abshire E, Stevens J, Epstein E, Loyola K, Rauscher M, Buchmann S
428   (2014) Honeybees (Apis mellifera) learn to discriminate the smell of organic compounds from
429   their respective deuterated isotopomers. Proc Biol Sci 281:20133089.
430   Haffenden LJW, Yaylayan VA, Fortin J (2001) Investigation of vibrational theory of olfaction with
431   variously labelled benzaldehydes. Food Chemistry 73:67-72.
432   Hallem EA, Carlson JR (2006) Coding of odors by a receptor repertoire. Cell 125:143-160.
433   Keller A, Vosshall LB (2004) A psychophysical test of the vibration theory of olfaction. Nat Neurosci
434   7:337-338.
435   Klika KD (2013) The Potential of 13C Isotopomers as a Test for the Vibrational Theory of Olfactory
436   Sense Recognition. ISRN Org Chem 2013:515810.
437   Kreher SA, Mathew D, Kim J, Carlson JR (2008) Translation of sensory input into behavioral output via
438   an olfactory system. Neuron 59:110-124.
439   Montague SA, Mathew D, Carlson JR (2011) Similar Odorants Elicit Different Behavioral and
440   Physiological Responses, Some Supersustained. J Neurosci 31:7891-7899.
441   Münch D, Galizia CG (2016) DoOR 2.0-Comprehensive Mapping of Drosophila melanogaster Odorant
442   Responses. Sci Rep-Uk 6:21841.

443 Münch D, Schmeichel B, Silbering AF, Galizia CG (2013) Weaker Ligands Can Dominate an Odor Blend
444   due to Syntopic Interactions. Chem Senses 38:293-304.
445 Palczewski K, Kumasaka T, Hori T, Behnke CA, Motoshima H, Fox BA, Le Trong I, Teller DC, Okada T,
446   Stenkamp RE, Yamamoto M, Miyano M (2000) Crystal structure of rhodopsin: A G protein-
447   coupled receptor. Science 289:739-745.
448 Paoli M, Anesi A, Antolini R, Guella G, Vallortigara G, Haase A (2016) Differential Odour Coding of
449   Isotopomers in the Honeybee Brain. Sci Rep-Uk 6:21893.
450 Pelz D, Roeske T, Syed Z, de Bruyne M, Galizia CG (2006) The molecular receptive range of an
451   olfactory receptor in vivo (Drosophila melanogaster Or22a). J Neurobiol 66:1544-1563.
452 Saberi M, Seyed-allaei H (2016) Odorant receptors of Drosophila are sensitive to the molecular
453   volume of odorants. Sci Rep-Uk 6:25103.
454 Schubert M, Hansson BS, Sachse S (2014) The banana code-natural blend processing in the olfactory
455   circuitry of Drosophila melanogaster. Front Physiol 5:59.
456 Silbering AF, Galizia CG (2007) Processing of odor mixtures in the Drosophila antennal lobe reveals
457   both global inhibition and glomerulus-specific interactions. J Neurosci 27:11966-11977.
458 Silbering AF, Okada R, Ito K, Galizia CG (2008) Olfactory Information Processing in the Drosophila
459   Antennal Lobe: Anything Goes? J Neurosci 28:13075-13087.
460 Silbering AF, Rytz R, Grosjean Y, Abuin L, Ramdya P, Jefferis GSXE, Benton R (2011) Complementary
461   Function and Integrated Wiring of the Evolutionarily Distinct Drosophila Olfactory
462   Subsystems. J Neurosci 31:13357-13375.
463 Solov'yov IA, Chang PY, Schulten K (2012) Vibrationally assisted electron transfer mechanism of
464   olfaction: myth or reality? Phys Chem Chem Phys 14:13861-13871.
465 Standfuss J, Edwards PC, D'Antona A, Fransen M, Xie GF, Oprian DD, Schertler GFX (2011) The
466   structural basis of agonist-induced activation in constitutively active rhodopsin. Nature
467   471:656-660.
468 Stensmyr MC, Dweck HKM, Farhan A, Ibba I, Strutz A, Mukunda L, Linz J, Grabe V, Steck K, Lavista-
469   Llanos S, Wicher D, Sachse S, Knaden M, Becher PG, Seki Y, Hansson BS (2012) A Conserved
470   Dedicated Olfactory Circuit for Detecting Harmful Microbes in Drosophila. Cell 151:1345-
471   1357.
472 Stranden M, Liblikas I, Konig WA, Almaas TJ, Borg-Karlson AK, Mustaparta H (2003) (-)-germacrene D
473   receptor neurones in three species of heliothine moths: structure-activity relationships. J
474   Comp Physiol A 189:563-577.
475 Turin L (1996) A spectroscopic mechanism for primary olfactory reception. Chem Senses 21:773-791.
476 Wang JY, Luthey-Schulten ZA, Suslick KS (2003) Is the olfactory receptor a metalloprotein? P Natl
477   Acad Sci USA 100:3035-3039.
478 Warne T, Serrano-Vega MJ, Baker JG, Moukhametzianov R, Edwards PC, Henderson R, Leslie AGW,
479   Tate CG, Schertler GFX (2008) Structure of a beta(1)-adrenergic G-protein-coupled receptor.
480   Nature 454:486-491.
481   -

482 Figure captions

483 Fig. 1

484 **Apparent differential responses to deuterated and non-deuterated benzaldehyde.** (A) Example of

485 responses to benzaldehyde-d_5 (green traces) and benzaldehyde-h (blue traces) at two different

486 dilutions (dashed: 10^{-3}, continuous 10^{-2}) in two areas of the antennal lobe (R1 and R2). The left

487   photograph indicates the position of R1 and R2 in the antennal lobe stained with the calcium sensor

488   GCaMP5, the middle graph depicts the response time-traces in area R1, the right graph R2. Gray bars

489   indicate stimulation times. Scale bar: 20 µm. (B, B') Spatial activity maps of the *Drosophila* antennal

490   lobe for the odorants E2-hexenal and ethyl butyrate, taken from the DoOR database,

491   http://neuro.uni.kn/door. (C) Spatial response patterns in the antennal lobe (false color)

492   superimposed onto the morphological view of the brain (grayscale). Responses to E2-hexenal, ethyl

493   butyrate, and the two benzaldehydes (BZA-h and BZA-d_5). Glomerulus DM1 innervated by dOr42b is

494   circled with a dotted line. The mid-line of the brain is to the left, and the orientation of the brain

495   corresponds to B. Scale bar: 20 µm. (D) Calcium recording from neurons expressing Or42b in the

496   DM1 glomerulus of the antennal lobe using the calcium sensor GCaMP6m. Stimuli were diluted to 10^{-2}

497    $^{-2}$. Ethyl butyrate elicited long-lasting responses, that did not resolve the temporal structure of the

498   double stimulus. Benzaldehyde-d_5 elicited clear excitatory responses (calcium increases), while

499   benzaldehyde-h elicited clear inhibitory responses (calcium concentration decreases) to each of the

500   two odor pulses. Mean $\pm$ s.e.m. (*N*=3 animals). (E): Coupled GC-antennal lobe recordings in

501   Or42b>GCaMP6m flies. The two bottom traces show the FID signal for the two benzaldehydes used,

502   the top panel shows the mean response $\pm$ s.e.m to benzaldehyde-h (concentration 10^{-2}, blue trace)

503   and benzaldehyde-d_5 (concentration 10^{-2}, green trace, *N*=3 animals). Both benzaldehydes show a

504   clear calcium decrease in glomerulus DM1 at the elution time of benzaldehyde (approx. 240 s), but

505   only benzaldehyde-d_5 shows a strong calcium increase at elution time around 100 s.

506   Fig. 2

507   **GC-Imaging recordings reveal minute impurities in commercial odorant sources.** Each panel shows a

508   GC-FID recording (red trace) and a simultaneous antenna calcium imaging trace from

509   Or42b>GCaMP6 flies (black trace). All odors were injected as headspace samples at 10^{-2} dilution. The

510   yellow bar indicates the elution time for ethyl acetate (100 s). A response in Or42b at that elution

511   time is present in several samples (left column), but other impurities were also found (see response

512   to ethyl butyrate). All traces: N=4-5, average $\pm$ s.e.m. For GC-FID traces, the error is smaller than the

513   line width. Bottom right: schematic of the experimental setup.

514   Fig. 3

515   **The impurity in benzaldehyde-d$_5$ is 0.0006% ethyl acetate.** (A): responses to different

516   concentrations of ethyl acetate in GC-Imaging of Or42b>GCaMP6 antennae (dilutions 10^{-10} to 10^{-2}).

517   Increasing concentrations are given in colors from orange-yellow to red. With increasing

518   concentration, the response increases in size, but remains at the same elution time of approx. 100 s.

519   At the highest concentrations, responses tail to the right. In gray, the response to 10^{-2} ethyl butyrate,

520   which gives four response peaks, the first peak likely due to presence of ethyl acetate. All responses

521   are normalized to the first response peak in ethyl butyrate. (B) Dose response curve to ethyl acetate

522   in GC-Imaging recordings. Peak responses are taken from panel A (dotted lines from the left).

523   Responses have been fitted with a sigmoidal dose-response curve, half-maximal response (EC50) is

524   reached at a dilution of $10^{-5.0}$. Green lines from panel C indicate the response intensities found there,

525   gray line the value of the first peak in the ethyl butyrate response. (C): GC-Imaging responses to our

526   samples of benzaldehyde-d$_5$ at a dilution of 10^{-2} (bright green) and 10^{-1} (dark green). At the elution

527   time of benzaldehyde (approx. 240 s) both samples elicit a prominent concentration dependent

528   calcium decrease. At the elution time of ethyl acetate (approx. 100 s) both samples elicit a strong,

529   concentration dependent calcium increase. Traces have been normalized to the response to ethyl

530   butyrate (gray trace). The concentration of the impurity can be extracted from the dose-response

531   curve in B (green lines) as $10^{-7.4}$ and $10^{-6.1}$, for 10^{-2} and 10^{-1} dilution, respectively. (N=3 animals).
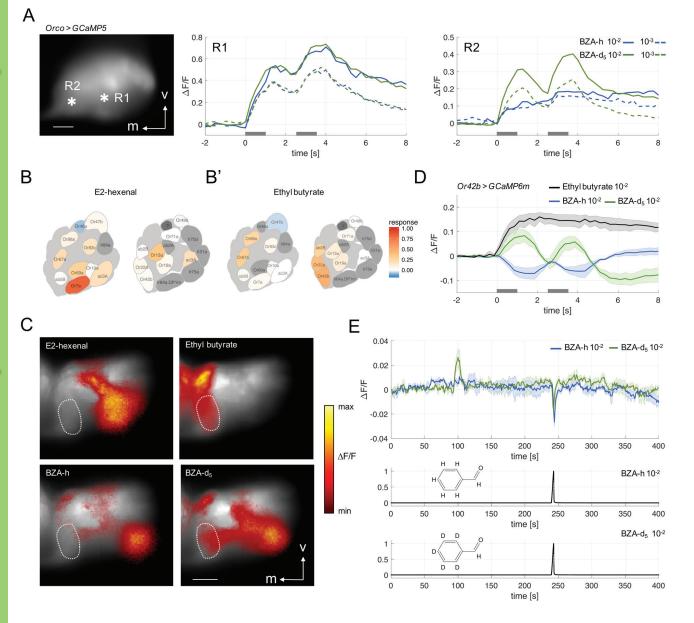
532   Fig. 4

533   **A minute impurity of ethyl acetate is sufficient to elicit a positive response to its mixture with**
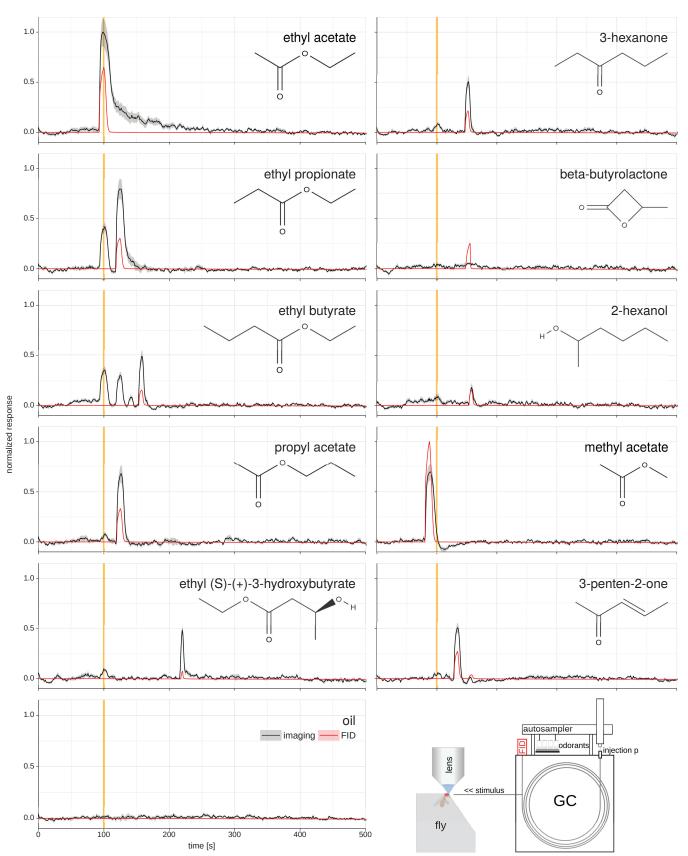
534   **benzaldehyde.** We recorded antennal calcium responses in Or42b>GCaMP6 flies. Responses to

535   benzaldehyde-h 10^{-2} were inhibitory. Gradually adding ethyl acetate in concentrations from 10^{-10} to

536   10^{-2} led to increasingly excitatory responses, in a dose dependent manner (color-scale, see inset; for

537   example, "0" in the legend means benzaldehyde-h at a dilution of 10^{-2}, "10^{-7}" in the legend means

538 that ethyl acetate at a dilution of 10^{-7} was added to benzaldehyde-h at dilution 10^{-2}, i.e. the relative

539 concentration was 10^{-5}). Gray: response to ethyl butyrate 10^{-2}, for calibration. Odors were pre-mixed

540 in mineral oil to mimic the contamination situation, and delivered with a PAL multisampler. All

541 traces: N=3, average $\pm$ s.e.m. Gray bars indicate stimulation times.

542